ICSO 2016

International Conference on Space Optics

Biarritz, France

18–21 October 2016

Innovative focal plane design for large space telescopes

Wilfried Jahn

Marc Ferrari

Emmanuel Hugot

Innovative focal plane design for large space telescopes

Wilfried Jahn, Marc Ferrari, Emmanuel Hugot

Aix Marseille University, CNRS, LAM (Laboratoire d'Astrophysique de Marseille)
UMR 7326, 13388, Marseille, France

wilfried.jahn@lam.fr

1   REVERSE IMAGE SLICER SOLUTION

Increasing the size of spatial telescopes is necessary to reach high resolution observation of the Earth, which implies more complex imaging systems in the focal plane. Not only physical dimensions are increased, but also relay optics are more numerous and complex. In order to reach high angular resolution and at the same time to keep a large field of view, the use of homothetic imaging systems as Spot and Pleiades satellites would lead to prohibitive linear focal plane dimensions. For infrared instruments used in space applications, the volume of the cryostat used to cool the detector is a dimensioning parameter for the lifetime of missions. By reducing the focal plane dimension, we may increase this lifetime and allow a significant decrease of the size of spatial systems.

As part of the CNES Research & Technology project, the main objective is in a first time to design a space telescope including an innovative arrangement of focal plane based on the Integral Field Unit (IFU) technology developed for ground based and space spectrometer (as for MUSE[1], SNAP[2], and NIRSpec[3] for the JWST). The idea is to consider the IFU principle in a reverse way, ie to subdivide the linear field of view with segmenting mirrors and re-image it on a 2D array detector to get wide field high resolution imager in a smaller volume.
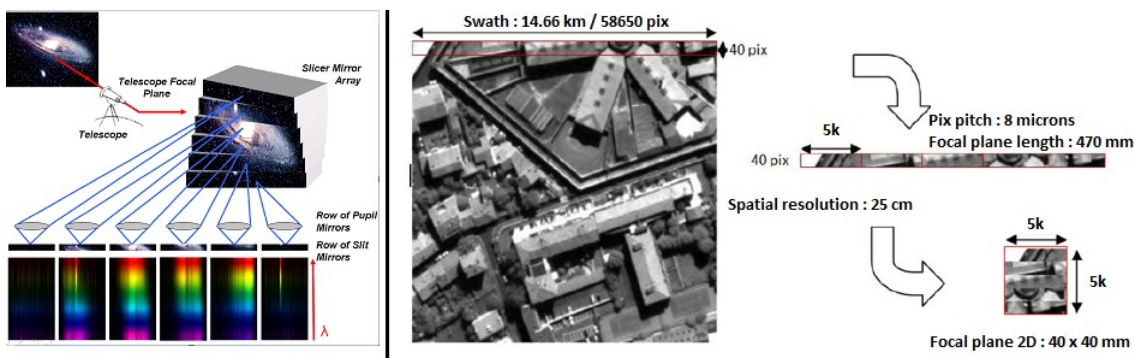

Fig. 1: [Left] The principle of an image slicer in spectrometer. The slicer mirror array, located at the image plane of the telescope, divides the entrance 2D field of view FOV and reimages the telescope exit pupils along a line on the pupil mirrors. Each pupil mirror then reimages its corresponding 1D slice of the entrance FOV on its corresponding slit mirror located at the spectrograph's focal plane. The reformatted FOV acts as the entrance slit in the spectrograph where all the slices are aligned as a pseudo long slit. [Right] The principle of a Reverse Image Slicer: The long linear FoV (red rectangle) is sliced in several sub-fields which are re-imaged on the top of the other on a matrix detector.

The main issue concerns the gap of field of view between an IFU device and a Earth observing telescope. According to the following Table 1, the telescope field of view is almost 1500 times higher than the IFU for SNAP or NIRSpec.

Angles of incidence on mirrors are very high, so it implies huge amount of field dependence aberrations like coma, astigmatism, field curvature and distortion. We propose an optical design based on freeform optics for the Image Slicer to correct such aberrations. We have increased mirror shape complexity step by step during the optimization until getting the best optical performance using only few polynomials. Zernike polynomials have been used for segmenting mirrors optimization from Z4 to Z13 according to Zemax definition. It is expressed by the following equation :

Table 1: Comparative table of two IFU characteristics for space missions and the Reverse Image Slicer device we propose.

	SNAP IFU	NIRSpec IFU	Reverse Image Slicer
Field of view [arcsec]	3 x 3	3 x 3	4320 x 115
Mirror shapes	Spherical tilted	Toroids tilted	Freeform
Number of sets of mirrors	3	3	2

$$z = \frac{c_x x^2 + c_y y^2}{1 + \sqrt{1 - (1+k_x)c_x^2 x^2 - (1+k_y)c_y^2 y^2}} + \sum_{i=1}^{N} A_i Z_i(\rho, \phi) \quad where \quad c_x = \frac{1}{R_x} \; ; \; c_y = \frac{1}{R_y} \qquad (1)$$

where z is the sag of the surface, c is the vertex curvature, k is the conic constant, and Z_i is the ith Zernike Standard terms with ρ the radial component in the aperture.

We present studies for a Korsch 1.3m F/22.4 telescope, covering a scan-field of 1.2°, with an accessible pupil plane. We consider two solutions: the first presents preliminary results with two sets of mirrors Image Slicer (IS) of magnification m = 1 and the second of magnification m = 2. The optical designs have been done by the software Zemax.

2   TELESCOPE AND REVERSE IMAGE SLICER MODULE CHARACTERISTICS

The telescope is composed by a 1.3m Korsch F_K / N and a module called "Image Slicer (IS)" of two sets of n mirrors. The IS has a magnification m, where the total focal length F_T is $F_T = m * F_K = 22.4m$. The matrix detector is a new generation matrix CMOS TDI detector 40x40 mm currently under development at CNES. A classical 1.3m Korsch is optimized in a first step without considering any Reverse Image Slicer (cf Figure 2). Indeed, it facilitates the telescope assembly process where a Korsch and an IS can be integrated and aligned independently before final assembly and characterization. An accessible pupil plane is required to set a deformable mirror based on Madras[4] project to compensate for thermo-elastic drifts as well as zero-gravity bending effects. It gives a complementary way of correction to motion compensation on M2 for the correction of undesired misalignment.
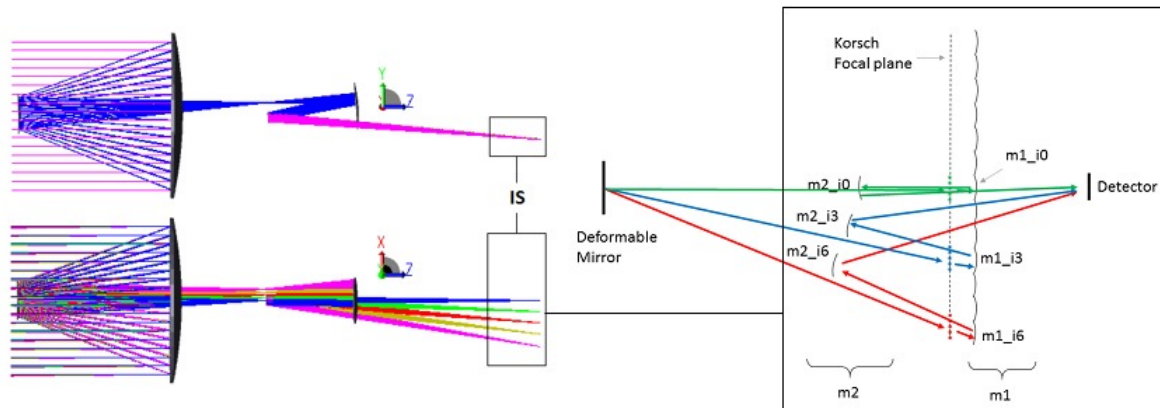

Fig. 2: [Left] Unfolded TMA Korsch telescope with a deformable mirror in pupil plane and the Image Slicer module location (Side and top view). [Right] The schema of the IS composed by a first set of segmenting mirrors m1 positioned after the Korsch focal plane, and a second set of focusing mirrors m2 re-imaging the 13 sub-images on the matrix detector. Three configurations are represented, it corresponds to the three sub-fields of optimization we consider for the following optical study.

Then an IS composed by two sets of freeform mirrors is added close to the Korsch focal plane to slice the 1D field of view and re-image each Korsch sub-images on a 2D 40x40 mm detector. It has a magnification m to reach the required spatial resolution on Earth. The cutting can be done before or after the Korsch focal plane to get some overlap between Korsch sub-images to facilitate final image reconstruction by image post-processing.

Two solutions have been investigated, each one is made of two sets of freeform mirrors. According to Table 2, higher the IS magnification, faster the Korsch and smaller its focal plane length is, so that the incidence angle on mirrors m1 and m2 are also decreasing. Even though a fast telescope is harder to realize and integrate, we assume at start it was easier to design an IS with lower angles of incidence on mirrors m1 and m2 to reduce their complexity, that's why we present two solutions where the magnification is the variable. On the next two sections, we present first optical results and compactness analysis for both solutions.

Table 2: Main system characteristics of the two Image Slicer solutions.

	Solution 1	Solution 2
Korsch focal length F_K [m]	22.4	11.2
Kosch F_K/#	17.2	8.6
Korsch linear image size [mm]	470	235
Image Slicer magnification m	1	2

3   REVERSE IMAGE SLICER MAGNIFICATION m = 1

The IS is composed by two sets of mirrors which slice the total field of view and image each sub-field with a magnification $m = 1$, corresponding to a Korsch focal length of $F_K = 22.4m$. It is made of :
- a set of 13 positive segmenting mirrors m1 after the Korsch focal plane which slice the 1.2° linear field of view in 13 sub-fields
- a set of 13 positive focusing mirrors m2 to form 13 sub-images on the detector

The surface map of mirrors m1 and m2 are defined by a set of Zernike polynomials, in order to simplify the optimization by giving more degrees of freedom. The distance between the Korsch focal plane and the mirrors m1 is defined by several parameters to get an overlap between each sub-image. We optimized over 3 configurations over the field: i0 (central-field), i3 (mid-field) and i6 (edge-field). Each configuration considers a sub-field of 0.1023° long. For the optimization of each configuration, we consider 5 field-points : one at the center, two at $\pm 0.7 * 0.05115°$, and two at $\pm 0.05115°$.

A   *Optical layout and mirrors characteristics*

Figure 3 shows the zemax models of the IS used for the optimization in the configuration where magnification is equal to 1. We obtain the following performance considering the Spot Diagram and Modulation Transfert Function.
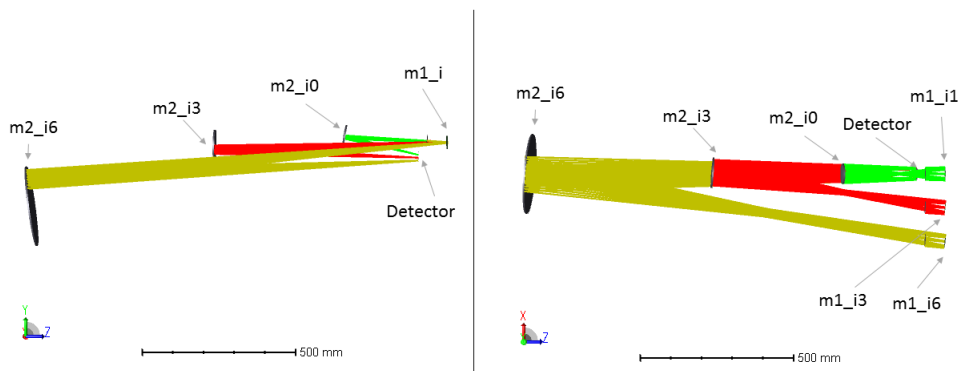

Fig. 3: Layout of the Image Slicer m = 1. Configuration i0, i3 and i6. Focusing mirrors m2 are positioned on the top of the other and close to the optical axis to minimize the astigmatism. [Left: Side view, Right: Top view]

Figure 4 represents sag surfaces of mirrors, it gives informations about the contribution of set of mirrors m1 and m2 to correct aberrations.

The peak to valley sag values are 0.911 mm for m1_i0, 0.467 mm for m1_i3 and 0.419 mm for m1_i6. The peak to valley sag values of focusing mirrors are 1.75 mm for m2_i0, 1.68 mm for m2_i3 and 5.57 mm for m2_i6. The deviation from the best sphere is still to be determined to characterize the freeform contribution on each mirror.
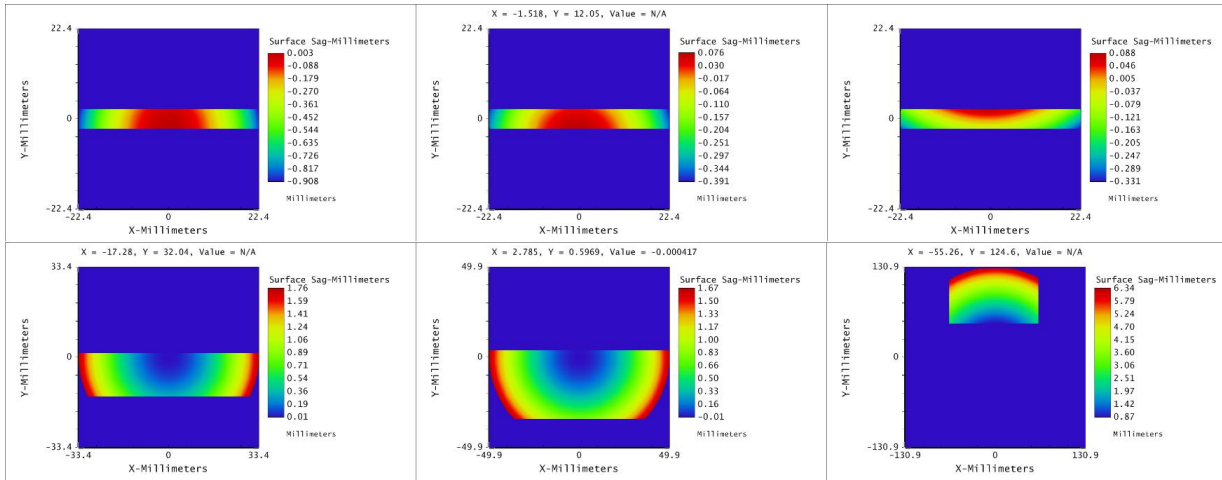
Fig. 4: Sag surface of mirrors. From left to right, configuration i0, i3 and i6. First line represents mirrors m1 and second line mirrors m2.

Table 3: Comparison of m1 and m2 mirror sizes for configurations i0, i3 and i6.

Configuration	i0		i3		i6	
Axis	X	Y	X	Y	X	Y
m1	44.8	5	44.8	5	44.8	5
m2	66.8	16	100	38	130	80

B   Optical performance
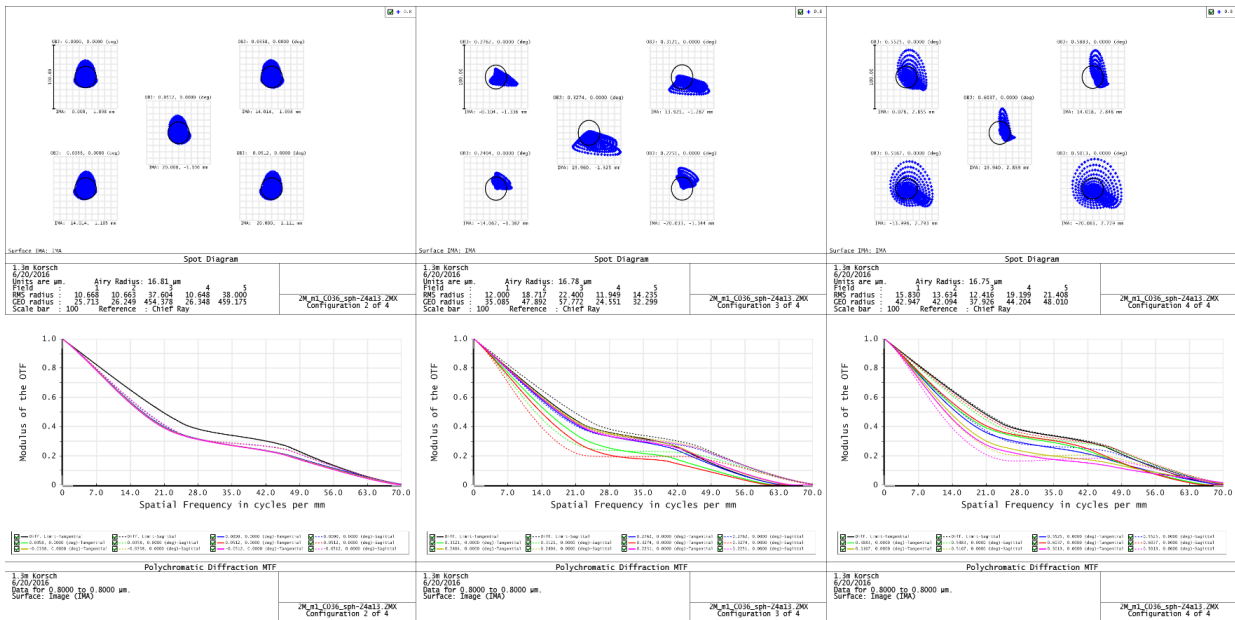

Fig. 5: Optical performance of Image Slicer m = 1. Form the left to the right, configuration i0, i3 and i6. We optimized over 5 field-points as described previously. We reach near diffraction limited performance, even if performance are slightly degraded over the field.

On the three configurations we obtain a near diffraction limited telescope. Residual aberrations remain by going through the field: coma, astigmatism and field curvature have to be corrected more precisely by different approaches described in the last section Discussion.

4   REVERSE Image Slicer magnification m = 2

The IS has a magnification m = 2, corresponding to a Korsch focal length of $F_K = 11.2m$.

A   Optical layout and mirrors characteristics
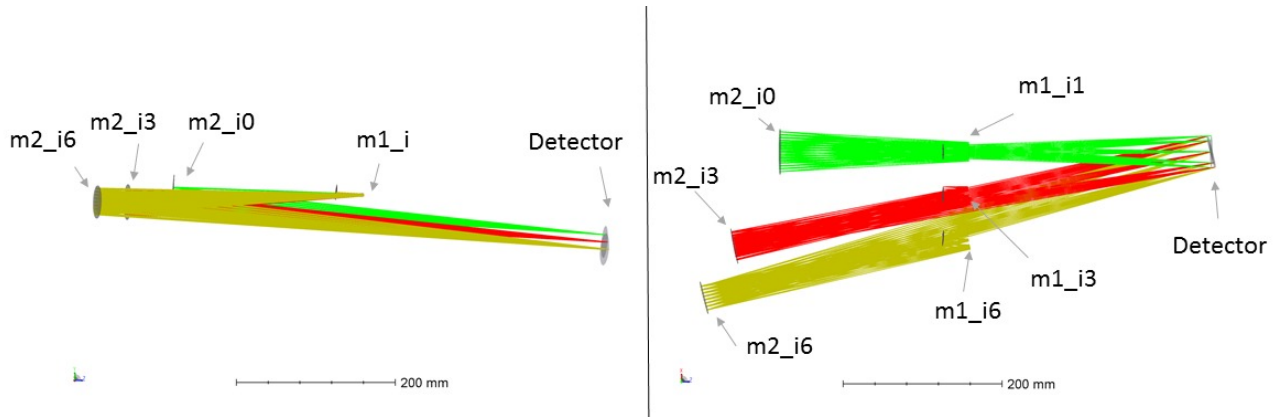
We optimized over the same three configurations.

Fig. 6: Layout of the Image Slicer m = 2. Configuration i0, i3 and i6. Focusing mirrors m2 are positioned next to each other to reduce angles of incidence which reduce astigmatism contribution on mirrors m2. [Left: Side view, Right: Top view]
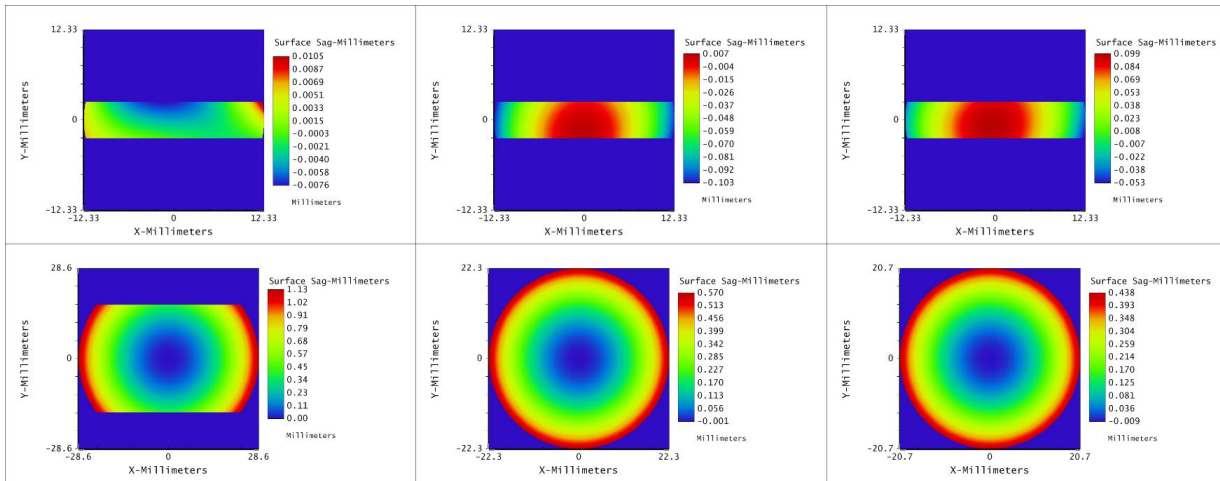

Fig. 7: Sag surface of mirrors. From left to right, configuration i0, i3 and i6. First line represents mirrors m1 and second line mirrors m2.

The peak to valley sag values are 0.018 mm for m1_i0, 0.110 mm for m1_i3 and 0.152 mm for m1_i6. The peak to valley sag values are 1.13 mm for m2_i0, 0.571 mm for m2_i3 and 0.447 mm for m2_i6. The deviation to the best sphere is still to be determined to characterize the freeform contribution on each mirror.

Table 4: Comparison of m1 and m2 mirror sizes for configuration i0, i3 and i4

Configuration	i0		i3		i6	
Axis	X	Y	X	Y	X	Y
Mirrors m1	24.6	5	24.6	5	24.6	5
Mirrors m2	57.2	34	44.6		41.4	

By comparing the Table 3 and 4 and the optical layouts, we observe two points:
- solution 2 has smaller mirror size by a factor 2 to 3 than solution 1

Solution 2 is interesting to get lighter and more compact system by increasing the magnification. Moreover, TDI linear detectors are already being used on space telescope (TRL9). However, it implies the use of several linear detectors instead of using only one matrix detector in solution 1.
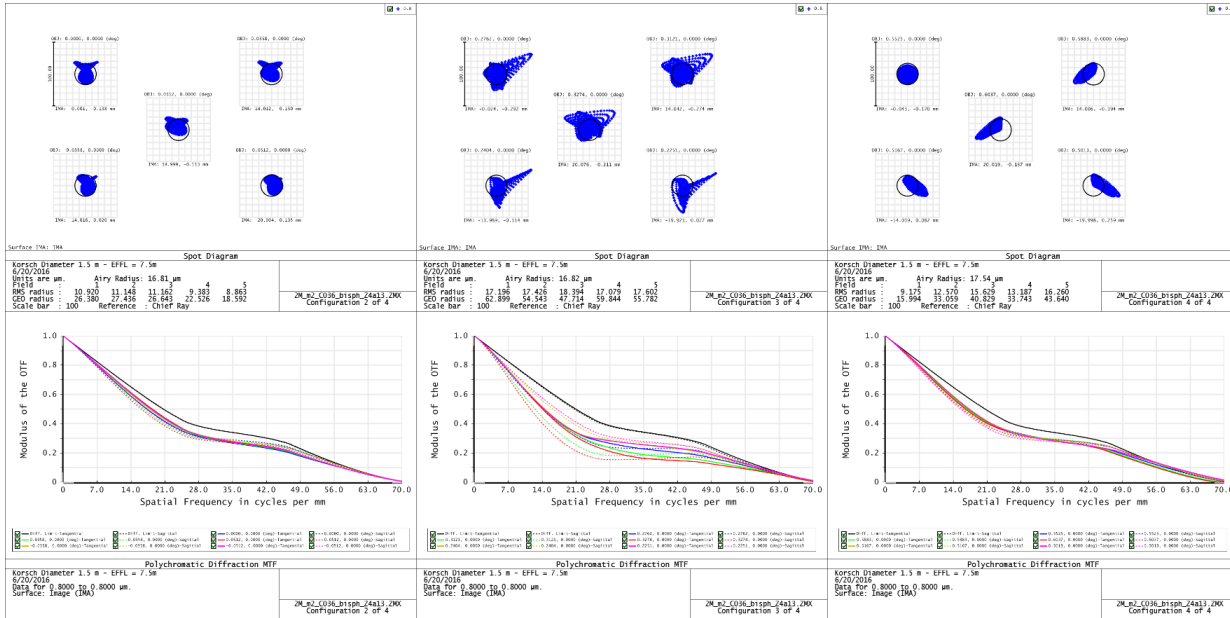
B   Optical performance

Fig. 8: Optical performance of Image Slicer m = 2. Form the left to the right, configuration i0, i3 and i6. We optimized over 5 field points as described previously. We reach near diffraction limited performance, even if performance are slightly degraded over the field.

Figure 8 presents optical performance considering the Spot Diagram and Modulation Transfert Function. It shows that on the three configurations we obtain a near diffraction limited telescope. Residual aberrations remain through the field: coma, astigmatism and field of curvature have to be corrected more precisely, as discussed in the final section.

The configuration i0 images perfectly a linear sub-image on the matrix detector. However, the sub-images of the configuration i3 and i6 are not co-linear with the configuration 1 : residual angles on the image position is $11.1°$ for i3 and $15.9°$ for i6 (cf Figure 9). Indeed, to reach such interesting results, it's better to reduce the tilt on m2 mirrors which concentrate the main part of aberrations (coma, astigmatism and especially field curvature). This is inappropriate to matrix detector, but the use of several linear TDI detectors already being used on space telescope may be more judicious for this solution. The idea would be to stack these linear detectors on the top of the other with different tilted positions. We could reach a compact focal plane composed by 9 detectors of 7000 pixels long.
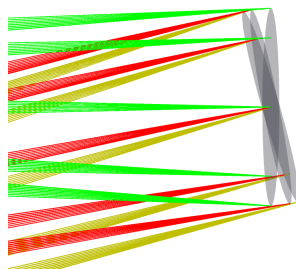

Fig. 9: Residual tilts between sub-images on the focal plane [green: configuration i0, red: configuration i3, yellow: configuration i6].

5   CONCLUSION

The emergence of innovative manufacturing technologies allows to envision optical designs using freeform mirrors. This approach revolutionizes the way optical designs are optimized, and offers new parameters of optimization.

In this article, we propose an optical freeform design of wide field high resolution planetary imager. Two Reverse Image Slicer optical systems at two different magnifications are compared in terms of optical performance and compactness for the ease of integration. Thanks to freeform mirrors, we can reach near diffraction limited planetary imaging telescope based on a drift-scan mode Korsch telescope by using a field slicer to reduce size and mass of the focal plane. The first solution represents an imager which slices a 1D field of view and re-image it on a 2D detector, while the second solution uses a stack of tilted linear detectors. This last solution is more compact and mirror size is smaller, these two points are a real issue and more efforts have to be done to reduce it. Manufacturing and alignment strategies would be an issue to be addressed in order to ensure a good optical quality.

Results obtained with Zemax are promising and give a trend on parameter values to improve the performance. Clearly, freeform mirrors are the core of this Image Slicer optimization to reduce the focal plane size without increasing too much the optical complexity.

Obviously, this study is the first step of future parametric studies. Several simulations are planned for the next. Considering both solutions :
- optimize the overall system (Korsch + Image Slicer) no more independently but like a global system
- find the best Image Slicer magnification m which minimizes the volume, allowing diffraction limited system avoiding too complex shapes of mirrors
- use more Zernike polynomials for the definition of mirrors m1 and m2

The second solution may also benefit curved linear detectors to correct more efficiently field dependent aberrations, especially the field curvature aberration. Indeed, the Laboratory of Astrophysics of Marseille (LAM, France) and the CEA Leti (France) works on Variable Curved Detector technology and are able to curve continuously from convex to concave VIS and IR matrix detectors[5][6]. This technology provides an other degree of freedom for the aberration correction (especially astigmatism and field curvature aberration) and would help this design to be more compact with simpler mirror shape.

References

[1] Henault, F., Bacon, R., Bonneville, C., Boudon, D., Davies, R. L., Ferruit, P., Gilmore, G. F., LeFevre, O., Lemonnier, J.-P., Lilly, S., Morris, S. L., Prieto, E., Steinmetz, M., and de Zeeuw, P. T., "Muse: a second-generation integral-field spectrograph for the vlt," *Proc. SPIE* **4841**, 1096–1107 (2003).

[2] Ealet, A., Prieto, E., and for the SNAP collaboration, "An Integral Field Spectrograph for SNAP Supernova Identification," *ArXiv Astrophysics e-prints* (Oct. 2002).

[3] Closs, M. F., Ferruit, P., Lobb, D. R., Preuss, W. R., Rolt, S., and Talbot, R. G., "The integral field unit on the james webb space telescope's near-infrared spectrograph," *Proc. SPIE* **7010**, 701011–701011–12 (2008).

[4] M., L., Hugot, E., Ferrari, M., Hourtoule, C., Singer, C., Devilliers, C., Lopez, C., and Chazallet, F., "Mirror actively deformed and regulated for applications in space: design and performance," *Optical Engineering* **52**, 091803 (Sept. 2013).

[5] Hugot, E., Jahn, W., Henry, D., and Chambion, B., "Flexible focal plane arrays for VIS/NIR wide field instrumentation," *Proc. SPIE* (2016).

[6] Tekaya, K., Fendler, M., Dumas, D., Inal, K., Massoni, E., Gaeremynck, Y., Druart, G., and Henry, D., "Hemispherical curved monolithic cooled and uncooled infrared focal plane arrays for compact cameras," *Proc. SPIE* **9070**, 90702T–90702T–8 (2014).